Developing microscopy based microfluidic SLS assay for on-chip hemoglobin estimation ⓕ

Lokanathan Arcot; Srinivasan Kandaswamy ✉; Anil Modali; ... et. al

Check for updates

CrossMark

View Online Export Citation

Articles You May Be Interested In

Hemoglobin estimation using ultra-low path length in microfluidic chips by quantifying Soret band

AIP Advances (July 2021)

Mössbauer studies of Fe^{2+} in anhydrous hemoglobin and its isolated subunits

J. Chem. Phys. (September 2008)

Electronic structure of Fe^{2+} in normal human hemoglobin and its isolated subunits

J. Chem. Phys. (August 2003)
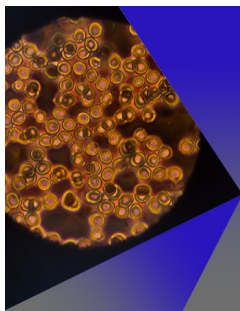
Developing microscopy based microfluidic SLS assay for on-chip hemoglobin estimation Ⓕ

View Online   Export Citation   CrossMark

Lokanathan Arcot,[1] ⓘD Srinivasan Kandaswamy,[1,a)] ⓘD Anil Modali,[1] Sai Siva Gorthi,[2] ⓘD
and Tathagato Rai Dastidar[1] ⓘD

AFFILIATIONS

[1] Sigtuple Technologies Pvt. Ltd., L-172, Sector 6, HSR Layout, Bengaluru, Karnataka 560102, India
[2] Optics and Microfluidics Instrumentation (OMI) Lab, Department of Instrumentation and Applied Physics,
  Indian Institute of Science (IISc), Bengaluru, Karnataka 560012, India

[a)] Author to whom correspondence should be addressed: srinivasan@sigtuple.com

ABSTRACT

Point-of-care (POC) biochemical assay is a highly important biochemical assay to estimate hemoglobin in the blood. High reagent volumes and complex-expensive optical setup requirements pose serious challenges when it comes to adopting conventional biochemical assays such as the Sodium Lauryl Sulfate (SLS) method into a POC device. Here, we report a modified SLS assay on a microfluidic platform, wherein the quantification is achieved using a simple microscopy-based imaging setup. Assay parameters, including SLS reagent-to-blood volume ratio, total reaction volume, the concentration of sodium dodecyl sulfate, and microfluidic chamber design, were optimized in order to achieve quantitation capability across a clinical range of hemoglobin using a path length suitable for the microfluidic platform. Besides quantitative correlation with a clinically accepted-validated standard method, the spectral absorption characteristics of the hemoglobin–SLS reagent mixture in the newly developed assay were compared with those of conventional SLS assays. The finalized chip design, including the reagent, cost 0.136 USD. The microfluidic chip in combination with an automated microscope was able to achieve a Pearson correlation of 0.99 in a validation study comparing the newly developed method and a commercially available hematology analyzer, with a turnaround time of 10 min, including incubation time. The clinical performance was ascertained, and the method achieved a sensitivity of 92.3% and a specificity of 53.8%. Overall, an automated microscopy-based biochemical assay was developed to estimate hemoglobin in whole-blood, using microfluidics technology, wherein the detector was a conventional camera associated with microscopy.

I. INTRODUCTION

Complete blood count (CBC) along with hemoglobin estimation is one of the most commonly performed preliminary medical diagnostic tests to ascertain the health of subjects. Hemoglobin level in blood is an important biochemical parameter indicative of a host of medical conditions, including anemia and polycythemia.[1] Hemoglobin estimation is almost always performed through photometric techniques. Naturally occurring hemoglobin consists of various chemical forms depending on the state of oxygenation or association with carbon dioxide, the oxidation state of Fe ion, and also biological variants depending on the specific types of sub-units making up the tetrameric hemoglobin molecule. The relative concentrations of these sub-types and forms of hemoglobin could vary significantly from person to person, also depending on the aging of the sample. It is worth noting that the spectroscopic absorption characteristics of these hemoglobin variants vary drastically.[2,3] As a result, an accurate estimation of hemoglobin, directly from the blood, requires absorbance measurements at multiple-wavelengths or chemical conversion of various forms of hemoglobin into just one form, thereby enabling single wavelength-based estimation of hemoglobin. The cyanmethemoglobin method is the gold standard for the colorimetric estimation of hemoglobin, but the Sodium Lauryl Sulfate (SLS) method is most widely used because of the benign nature of reagents involved compared to the former.[4] Sodium dodecyl sulfate (SDS) is the active ingredient responsible for chemical

conversion of various forms of hemoglobin into the methemoglobin–SLS complex at concentrations of SDS used in conventional SLS assays (2 mM), as reported by Oshira et al.[5] Clinical and point-of-care (POC) hemoglobin devices capable of performing cell count as well as hemoglobin estimation often use separate optical systems to derive quantitative information. Imaging-based cell counters use a camera as a detector, whereas colorimetric hemoglobin estimation is generally performed using dedicated high sensitivity photodetectors.

All techniques used in the estimation of hemoglobin in the blood can be classified into invasive and non-invasive. Non-invasive techniques, though very convenient because of the absence of needle prick, suffer from inferior performance; therefore, these techniques are almost always used as screening tools.[6–8] Most widely prevalent commercially available point of care hemoglobinometers are fundamentally spectrophotometers that measure absorbance at one or more wavelengths, with or without lysing out the RBCs.[8] One major limitation of these commercially available hemoglobinometers is their exclusive functionality and an alternative to these are mobile phone camera-based devices, which often work in conjunction with the microfluidic Lab-on-Chip (LOC) platform. Microfluidic technology enables reagent and sample volume minimization; additionally, a higher extent of automation becomes possible, thereby minimizing errors from manual steps. Because of miniature path lengths, microfluidic chips often require high sensitivity detectors. For example, a report from Steigert et al.[9] used a spinning disk with a 5 mm wide chamber to detect hemoglobin using green LED (532 nm) illumination, spectroscopy detector, with a total internal reflection facility, which enabled the path length along the width of the chamber instead of height and spinning action allowed mixing. Using the SLS reagent (1:49 blood:reagent volume ratio), they were able to achieve an R^2 of 0.993 (correlation with true values of hemoglobin in blood samples) and a lower limit of detection of 0.29 g dl^{-1}.[9] This conclusion was based on five blood samples, and also the clinical performance was not ascertained, most probably because of the small sample size. In a very similar study by Wu et al.,[10] a 100 μm microcuvette was used, which had the dried SLS reagent, and the mixing of reagent and blood occurred spontaneously without active mixing. Illumination and detection were achieved using a green LED (540 nm) and a photodiode, respectively.[10] With this setup, they reported an R^2 of 0.945, which was calculated based on five blood samples, again without clinical performance analysis. The majority of hemoglobin measurements are often accompanied by quantification of a host of other blood-related parameters, collectively known as complete blood count (CBC), which is derived using commercially available hematology analyzers. Even though hematology autoanalyzers perform multiple measurements, they are expensive and also not suitable for POC applications. When it comes to developing POC technologies to provide CBC, imaging-based artificial intelligence (AI) supported technologies are becoming increasingly popular.[11]

A disadvantage of using a separate detector-illumination setup for hemoglobin estimation, besides the setup associated with an imaging-based differential cell counting, would be the requirement of additional optical elements such as a beam splitter, separate optical column, an extra objective of suitable magnification, and also additional hardware–software provisions. Therefore, utilization of dedicated detectors would result in devices with narrow

applications, for example, just hemoglobin estimation and nothing else.[12] Therefore, an ideal imaging-based POC medical device for CBC should use the same optoelectronic setup for hemoglobin estimation. In a report by Nikita et al.,[13] a PDMS microfluidic device with a chamber depth of 50 μm was used in combination with a 540 nm green LED for illumination and a CMOS camera. Using this imaging-based setup, they demonstrated a linear relationship between measured OD and hemoglobin concentration up to 8 g dl^{-1}, without using any lysis reagent.[13] Performance evaluation indicated that the accuracy was satisfactory to diagnose severe anemia, whereas it was not suitable for estimating hemoglobin in blood samples with normal and abnormally high hemoglobin concentrations. Hongying et al.[14] reported a correlation of R^2 0.92 with commercial autoanalyzer derived hemoglobin values, using a mobile phone camera in conjunction with a 430 nm blue LED and 1 cm cuvette.[14] The blood samples were lysed using a commercially available lysing reagent and subsequently loaded into the cuvette, which was placed in the holder for automated imaging followed by analysis for estimation of hemoglobin. However, this was not performed on a microfluidic platform, and they used three separate add-on and three separate chambers for estimating hemoglobin, RBCs, and WBCs, which leads to a complicated setup with regard to usability.

Here, we report the development of microscopy imaging-based estimation of hemoglobin in blood using the same optical setup associated with estimating differential as well as total counts of white blood cells in blood smears. The imaging microscopy-based hemoglobin estimation required the development of a microfluidic chip along with optimization of the SLS reagent to enable quantitative estimation of hemoglobin across the required clinical range. Photodetectors, such as CCDs and APDs, are widely used in POC medical devices associated with colorimetric assays, whereas cameras associated with microscopes are not as popular. Additionally, the signal recorded from conventional SLS assay protocols would be extremely low when compared to cuvette-based measurements because of small path lengths associated with the microfluidic setup, thereby necessitating a dedicated detector.[15] In order to compensate for low sensitivity and low signal intensity, the volume ratio between blood and the SLS reagent, as well as the concentration of SDS in the SLS reagent, was modified so as to enable sensitivity for hemoglobin across the clinically relevant range on an automated microscopy setup. The reagent optimization was initially performed using a clinical chemical analyzer, which measured absorbance at 546 nm. The thus developed LOC compatible SLS reagent was further spectroscopically characterized using a nanospectrophotometer, and the peak positions corresponding to hemoglobin–SLS complex were compared with those observed in the case of conventional SLS assay reagent used in clinical labs in conjunction with the clinical chemical analyzer, such as Erba Chem 5×. The characteristics of the microfluidic chip, including the height of the chamber (or path length), the length, and the width, were optimized so as to enable a statistically satisfactory quantitative correlation between ground truth and the value obtained from in-house developed microfluidic chip in conjunction with an automated microscopy device. In order to achieve the necessary narrow-band illumination in the green region, which is needed for SLS assay, an RGBW LED was used with just the green LED activated.

In the present work, the development of reagent composition along with the optimization of parameters of the microfluidic chip

was performed initially using hemoglobin standards prepared in-house from lyophilized hemoglobin, followed by verification using whole blood samples. Overall, we present the results of a study involving microscopy imaging-based estimation of hemoglobin in blood using a microfluidic chip, wherein the photometric quantification was performed on an automated microscope designed to provide complete blood count and differential count. Here, the advantage is common illumination and a detection system between the cell imaging setup and the hemoglobin estimation setup.

II. MATERIALS AND METHODS

A. Chemicals

Sodium dodecyl sulfate (SDS), Triton X-100, lyophilized human hemoglobin, PBS buffer tablets, and Pluronic F-127 were procured from Merck-Sigma-Aldrich, Bangalore, India. All chemicals were used in experiments as supplied without any further purification or modification. Type II deionized water (resistivity 15 MΩ) dispensed by Milli-Q HX was used for all reagent preparation purposes.

B. Equipment

The SLS–blood/Hb standard solutions were analyzed using Erba Chem 5× clinical chemical analyzer, and for hemoglobin estimation, the recommended settings with absorbance measurement at 546 nm were used. All UV–vis absorption measurements were performed using the NanoPhotometer NP 80, IMPLEN, Germany. The hemoglobin concentrations of both blood samples and in-house prepared hemoglobin standard solutions were measured using a commercial hematology analyzer (Sysmex XP-100). The in-house built digital scanner was used to record images of the microfluidic chamber filled with the blood/Hb standard–SLS reagent mixture. The digital scanner consisted of the following hardware components:

- Computer system: A mini-ATX motherboard with Intel i5 quad-core processor, 8GB RAM, NVIDIA GPU with 4G GPU memory, running Ubuntu Linux (v16.04).
- Optics system: An optical tube (40× Plan Achromat objective and 10× eyepiece) and an Abbe condenser with RGBW LED source. A 13MP USB 3.0 color camera procured from e-con Systems, Inc., USA, was used. The camera model See3CAM_CU135 contained a 1/3.2 AR1335 CMOS image sensor from ON semiconductor. During the hemoglobin measurement, only the green LED was active. An RGBW LED model XLamp® XM-L® Color LED procured from Cree, Inc., USA, was used to achieve green illumination.
- XYZ slide stage: The XYZ platform was built using commercially available low-cost ball screws and stepper motors, along with some machined parts.

C. Methods

1. Preparation of hemoglobin standard solution from lyophilized hemoglobin

Lyophilized hemoglobin powder was used to prepare standard solutions. Lyophilized Hb powder (200 mg) was added to 1 ml PBS and mixed to ensure dissolution of hemoglobin. After sufficient mixing, the tube with the hemoglobin solution was allowed to stand for 10 min to let undissolved residue particles settle down, and subsequently, two distinguishable layers were formed: an upper clear layer consisting of dissolved hemoglobin and a lower layer made up of undispersed, undissolved aggregates. The upper layer was carefully pipetted out, which was analyzed using a Sysmex XP-100 hematological analyzer to ascertain the concentration of hemoglobin. This resulting stock solution was serially diluted further to give hemoglobin standard solutions with lower concentrations, and subsequently, these standard solutions were analyzed for hemoglobin concentration by Sysmex XP-100. The concentrations of hemoglobin in the in-house prepared hemoglobin standard solutions are presented in Table I.

2. Preparation of modified SLS reagent

The procedure for estimating hemoglobin in the blood through conventional SLS assays was adopted from a report by Oshira et al.[5] The composition of the SLS reagent consisted of 2.5 mM SDS, 1.1 mM Triton X-100, and 0.08 mM PBS. As explained in the Introduction, the assay format including the composition of SDS had to be modified in order to compensate for the low signal and sensitivity, if the conventional SLS assay were to be performed on a microfluidic setup in conjunction with a camera-based detection system. SDS is the active ingredient in the SLS reagent responsible for the chemical transformation of hemoglobin into methemoglobin–SLS complex. Therefore, the concentration of SDS was varied to conduct a modified SLS assay involving variation in blood:reagent volume ratio. The SLS composition used in conventional SLS assays was denoted as 1× SLS (2.5 mM). Modified SLS reagents containing 10 times (25 mM), 50 times (125 mM), 100 times (250 mM), and 240 (600 mM) times higher SDS concentration than 1× SLS are denoted as 10× SLS, 50× SLS, 100× SLS, and 240× SLS, respectively. The blood:reagent volume ratio in conventional SLS assays is 1:250. In order to increase the concentration of the hemoglobin–SLS complex, the blood:SLS volume ratio was increased from 1:250 to 1:25 and 1:5.

3. Effect of SDS concentration and blood:SLS volume ratio

As mentioned in earlier sections, in order to adopt conventional SLS assay onto microscopy-based microfluidics platform,

TABLE I. The results of hemoglobin concentrations in standard solutions prepared in-house by dissolving lyophilized hemoglobin in PBS, followed by analysis using the Sysmex XP-100 hematological analyzer. The R^2 for linear correlation was found to be 0.99.

Hb. conc. (g dl^{-1})	Lyoph. Hb. (g dl^{-1})
18.6	30
13.2	20
11.7	18
10.7	16
9.2	14
7.9	12
6.7	10
6.7	8

parameters such as blood:SLS volume ratio and SDS concentration had to be optimized. The quantitative estimation of change in absorbance in the wavelength range relevant to SLS assay with the modified SLS reagent (10× SLS, 50× SLS, 100× SLS, 240× SLS) and modified volume ratio (1:25, 1:5) was performed using an Erba Chem 5× chemical analyzer, which estimates hemoglobin by measuring absorbance at 546 nm. The absolute value of absorbance was used to identify the optimal SDS concentration in the SLS reagent and also optimal blood:SLS volume ratio. These optimized parameters enabled the highest enhanced signal to distinguish anemic and non-anemic samples. Initial optimization experiments were performed using in-house prepared hemoglobin standard solutions, and once the reagent parameters were optimized, the signal enhancement was also confirmed with a whole blood sample.

4. Comparing spectral absorbance of 1× SLS-Hb std mix and 50× SLS-Hb std mix

The chemical transformation of various forms of hemoglobin upon addition of 1× SLS reagent to blood is well understood and the conversion to methemoglobin followed by the formation of a complex with SLS forms the fundamental basis of conventional SLS assays. It is important to ensure that the chemical transformation of hemoglobin happening in the modified SLS assay is similar to that taking place in the case of conventional SLS assay performed using 1× SLS reagent. After preliminary on-chip experiments, 50× SLS, along with 1:5 blood to reagent volume ratio was found to be suited to efficiently distinguish anemic samples from non-anemic samples. Hence, this reagent format was chosen to compare the important spectral characteristics, including peak positions of the Soret band and the Q band. Even though only the Q band peak is used for quantification purposes, the Soret peak position is also considered an important spectral characteristic of conventional SLS assays. Thus, the peak positions of these two peaks were compared in order to confirm the similarity between the conventional SLS assay and the modified SLS reagent developed during this study.

5. On-chip photometric estimation of hemoglobin using an automated microscope

The AI-powered digital scanner was designed such that it could operate under two modes relevant to blood analysis, the first mode was for identifying and counting cells/platelets in a mixture of blood and necessary reagents loaded into a microfluidic chamber. It must be noted that the automated microscope used here has the capability to operate under multiple other modes including the ones to analyze urine and semen. Among the blood analysis related modes, the first mode would generate white light using the RGBW LED, and the AI-powered auto-focus program would enable capturing well-focused images at specified locations in the region of interest within the two-dimensional area of the microfluidic chamber or a smear slide. The details of this focusing algorithm can be found in the report by Dastidar and Ethirajan.[16] The second mode was for estimating the hemoglobin content, and this activated only the "Green" part of the RGBW LED. A schematic representing various sections of the setup associated with the second mode is presented in Fig. 1. As shown in the schematic, the overall system consists of a multi-chambered microfluidic chip filled with the SLS–sample mixture,
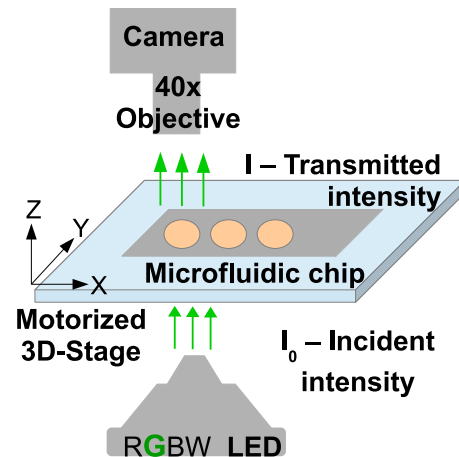

FIG. 1. Schematic of the overall setup used in association with a microfluidic chip for estimating hemoglobin in the blood. Totally three parts, first the imaging part consisting of camera and objective. Next, a motorized XYZ slide stage for moving the chip into the imaging plane and finally the illumination part consisting of the "Green" activated RGBW LED.

held by a motorized stage. The chip is placed in between a green light source (which consists of an LED, iris diaphragm, and condenser) and a camera that receives light from the chip via a 40× objective. As mentioned in Sec. II C 4, the Q band of the SLS–hemoglobin mixture is most critical to estimating hemoglobin using the SLS assay. The Q band has a peak at 535 nm; hence, an assessment was necessary to check if the "Green" part of RGBW LED was suited for the estimation of hemoglobin. The specification sheet of the LED indicated that the "Green" emission had a peak at 520 nm, and we experimentally measured the intensity at 535 nm, which was 20% less than that at 520 nm. Based on preliminary experiments (data not shown), it was concluded that the "Green" part of the RGBW LED was capable of providing good sensitivity to classify blood samples into clinically relevant categories, as mentioned in Table II.

Several parameters associated with the optical setup were optimized to achieve optimal sensitivity across the clinical range of hemoglobin. Camera related parameters included exposure, gain, white balance, and local tone mapping. The specific details about the fabrication procedure involved in making the microfluidic device needed to measure the hemoglobin concentration in blood

TABLE II. Reference table for classifying blood samples based on hemoglobin values grouped into clinically relevant ranges depending on the therapeutic action needed.

S. no.	Hb range (g dl^{-1})	Medical condition
1	<7	Anemic, requiring transfusion
2	7–12 (men), 7–13 (women)	Anemic, no transfusion required
3	12–16.5 (men), 13–16 (women)	Normal
4	>16 (women), >16.5 (men)	Polycythemia

are described in Sec. II C 6. Preliminary experiments were performed to optimize the physical parameters, including chamber depth and lateral dimensions/design, and the details are presented in Sec. II C 6. Once the reagent–sample mixture filled microfluidic chip was placed on the motorized stage, the chip was moved along all three dimensions such that the first chamber's base was brought into focus. The "X" and "Y" coordinates were predetermined and stored in the memory of the computer, while the "Z" focal plane for each chamber was arrived upon using an AI-powered auto-focus algorithm.[16] To start with, the entire chip was placed significantly farther away from the objective associated with the camera, as shown in Fig. 1. The imaging plane was brought closer to the base of the chamber by moving the chip closer to the objective, along the "Z" axis. Based on the feedback obtained from live images generated by the camera, the "Z" movement of the stage is stopped at the position where the base of the chamber comes into focus. Initial studies indicated that the milling marks at the base of the chamber significantly altered the grayscale values. Therefore, once the ideal focal plane was determined, the imaging plane was moved into the chamber away from the base (the chip is moved closer to the objective per schematic in Fig. 1) so as to eliminate the contribution from milling marks. Overall, for each chamber, multiple images were recorded at the first field of view (FOV), and an AI model was used to derive the ideal focal distance, followed by moving away from the base of the microfluidic chamber by a fixed distance of 240 μm. After moving the imaging plane by 240 μm at the first FOV, 11 images were recorded within the 3×3 mm^2 area at the center of each chamber. This entire process was repeated for two other chambers. In all, each sample was mixed with the SLS reagent followed by loading into a chip containing three interconnected chambers, wherein each chamber was 1.3 mm deep and 7 mm in diameter. Using just the "Green" of RGBW LED, 11 images were recorded per chamber, totaling 33 images for each microfluidic chip.

Even though each image was 13 megapixels in size, only a subset of that was found to be ideal for extracting gray level value from each image captured in the green channel of the camera. We used the median of a 512×512 pixel^2 patch at the center of each image to extract the gray level value. Subsequently, the median of gray level values from 11 images of each chamber was calculated. Further, an average of three gray level values obtained from three chambers was calculated, and this value was used as the intensity in the following two step calculation to estimate the hemoglobin concentration in blood or hemoglobin standard.

 a. *Step 1 calculation.*

$$Hb\ Conc. = \frac{\log\frac{Io}{I}}{pathlength \times ext.\ coeff.}, \tag{1}$$

$$Hb\ Conc. = \frac{\log\frac{Io}{I}}{0.13 \times 2.797}, \tag{2}$$

where I is the gray level value obtained from three chambers, and Io the pre-measured value corresponding to gray level obtained from chambers filled with the SLS reagent (no blood). Here, the extinction coefficient has a unit dl g^{-1} cm^{-1}, so that upon calculation, the output concentration is in the clinically relevant range g dl^{-1} instead of molarity.

The hemoglobin values obtained from step 1 were correlated with ground truth values and curve fit (Power fit) was performed. The correlation equation thus obtained was used as a calibration equation to convert the Hb value from step 1 into the final Hb concentration. With the specific setup, the following correlation equation was obtained:

 b. *Step 2 calculation.*

$$Final\ Hb\ conc. = 12.65 \times (output\ step1)^{0.76}. \tag{3}$$

The details regarding the experimental deduction of constants involved in steps 1 and 2 are discussed in the results section.

6. Design and fabrication of microfluidic chip for Hb estimation

To estimate hemoglobin concentration in a microfluidic platform, a three chamber device was designed. The specifics of the design, including the dimensions, are presented in Fig. 2. After initial experiments using single-, double-, and three-chamber design, it
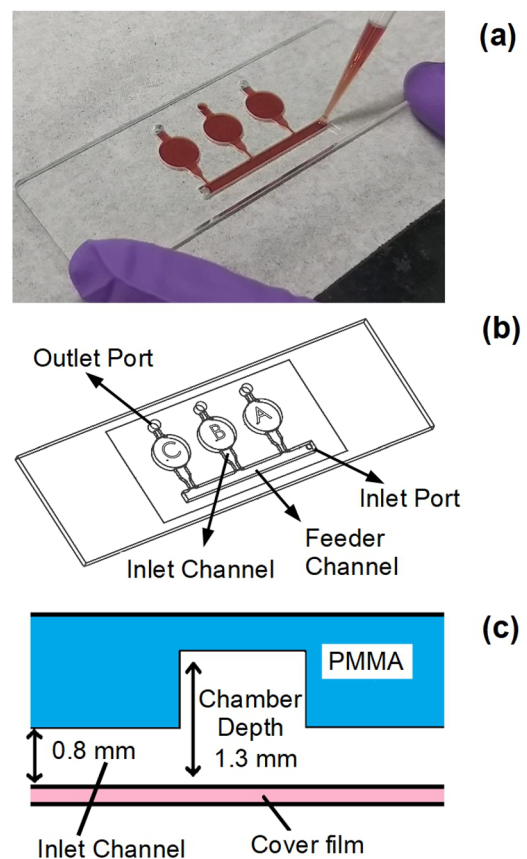

FIG. 2. Various aspects of the microfluidic chip design. An actual microfluidic chip filled with the blood–reagent mixture (a), schematic representation of chip-sized 75×25 mm^2, having three interconnected chambers with various parts labeled (b) and the cross section across the inlet channel through the chamber showing respective depths (c).

was observed that a three-chamber design resulted in best accuracy with regards to estimating the concentration of hemoglobin. This improved accuracy was a result of increased sample size, thereby minimizing the contribution from outliers. A time-lapse image series of a microfluidic device being filled with a blood–reagent mixture is presented in Fig. 13 in the supplementary material. Each chamber was 7 mm in diameter and 1.3 mm deep.

The microfluidic chip for HB detection was designed to have a single inlet through which the blood–reagent mixture is flowed using a pipette. The sample inlet port has a diameter of 1 mm so that the pipette tip fits in tightly, thereby preventing any possible leak. Each of the three chambers has vent ports to let the air escape during the filling process. In the future, a drain channel connecting all three outlets would be added to prevent the sample–reagent mixture from leaking out of the three vent ports. The sample–reagent mixture is filled into three chambers by forcing the liquid with the help of a pipette-tip inserted into the 1 mm wide inlet port. From Fig. 2(b), it can be observed that chamber A is closer to the inlet port as compared to chambers B and C. This configuration will result in the filling of chamber A first. Further application of pressure will cause the blood–reagent mixture to leak at the outlet port of chamber A and do not allow the blood mixture to fill the other chambers. Hence, the device was designed such that the fluid fills the feed channel first followed by simultaneous filling of all three chambers. In order to achieve this, the hydraulic resistance of the feed channel should be lower than the hydraulic resistance of inlet channels of all three chambers. Assuming that the fluid is continuous and the flow is laminar, the hydraulic resistance of a microchannel can be calculated according to Eq. (4). Here, μ is the viscosity of the fluid, L is the length of the microchannel, w is the width, and h is the height of the microchannel.[17] It can be observed from Eq. (4) that the hydraulic resistance of the channel is inversely proportional to the cube of channel height. Hence, the hydraulic resistance of the feed channel was designed such that its resistance was less than that of the inlet channels of the chambers by a factor of three. This would eventually fill three chambers simultaneously as they were designed such that the hydraulic resistance balances the flow front of the blood mixture,

$$Resistance \approx \frac{12 \times L \times \mu}{w \times h^3}. \qquad (4)$$

A time-lapse image series of the process of blood–reagent mixture filling the microfluidic chip is presented in Fig. 13 in the supplementary material. Overall, the sample loaded at the inlet port fills the feeder channel first and then passes through the chamber inlet channels to subsequently fill the imaging chambers. It is critical that the chamber does not contain any bubbles or air column during the filling process. It was found that the air gets trapped in the imaging chamber when the height of the inlet channel is less than half of the height of the imaging chamber. Since the height of the imagining chamber was 1.3 mm (maximum height possible on a 1.5 mm thick PMMA sheet), in order to avoid air column formation, the height of the inlet channel should be >0.65 mm. Per this requirement, the height of the inlet channel was chosen to be 0.8 mm in the finalized design. Additionally, it was observed that air got trapped at the corner due to the inability of the fluid to wet the surface at the corners of the chamber. In order to mitigate this, the wettability of the PMMA surface was improved by surface modification. The details of surface

treatment can be found in the following paragraph describing the fabrication and assembly process.

The desired pattern was designed using the program Autocad, and the design file was provided as input to the machining software (Mach 3). The specific milling parameters, namely, spindle rpm, feed rate, and depth of cut, were provided as inputs. A 100 μm end mill was used to mill the design pattern on (75 × 25 × 1.5 mm^3) PMMA sheets, using a CNC micromilling machine (Minitech Machinery, USA). The milled three chamber device was geometrically characterized using vernier caliper (length, width, and thickness) and digital screw gauge (depth). The fabricated device was used for assay purposes only if dimensions (length, width, and thickness) were within a tolerance of ±200 μm. The tolerance for the depth of the chamber was ±15 μm. After characterization, the device was cleaned using soap solution (extran) in an ultrasonicator bath and rinsed with DI water. In order to minimize the formation of air columns in chambers, the milled-cleaned PMMA devices were coated with polymeric surfactant [poly(ethylene glycol)-block-poly(propylene glycol)-block-poly(ethylene glycol)], known by the trade name Pluronic F127. Briefly, the milled-cleaned PMMA slides were immersed in 1M nitric acid for 1 h, followed by a rinse with DI water and blow-drying using nitrogen. Subsequently, the device was immersed in a 0.5% (w/v) aqueous solution of Pluronic F 127, for 30 s, followed by drying in a hot air oven at 65 °C for 1 h. Finally, the fabricated pattern was enclosed uniformly with 9793R (3M, USA) hydrophilic single-sided transparent cover film using a laminator (GBC Catena, USA) in class 100 000 cleanroom.

7. Workflow for conventional and modified microfluidics compatible SLS assay

The conventional SLS assay was performed as per procedure reported by Oshiro et al.[5] Briefly, 20 μl whole blood (EDTA treated) or in-house prepared hemoglobin standard solution was added to 5 ml 1× SLS reagent in a test tube and mixed ten times, followed by incubation for 10 min. Subsequently, the absorbance measurement was performed within 1 h (from the time point of mixing blood and reagent), either using a biochemical analyzer (Erba Chem 5× clinical chemical analyzer) or nanospectrophotometer. In the case of studies pertaining to customizing and understanding the modified SLS assay using biochemical analyzer or nanospectrophotometer, required volume of blood/hemoglobin standard solution (calculated based on volume ratio) was added to 600 μl SLS reagent, followed by mixing ten times, followed by incubation for 10 min. Subsequently, the absorbance measurement was performed within 10 min–20 min window from the time point of mixing blood and reagent. The time window of measurement was deduced based on preliminary studies using nanospectrometer, wherein the absorbance of SLS–blood mixture was measured for up to 1 h (data not shown), and it was observed that during the 10 min–20 min time window, the absorbance remained stable, but beyond 25 min, the absorbance value gradually increased.

Once various SLS concentrations, along with different volume ratios were studied, 50× SLS and blood:reagent volume ratio 1:12 were finalized, and a procedure was arrived upon to perform clinical verification using 30 blood samples, with at least five samples each in clinically relevant ranges mentioned in Table II. In order to obtain samples with hemoglobin concentrations less than 7 g dl^{-1},
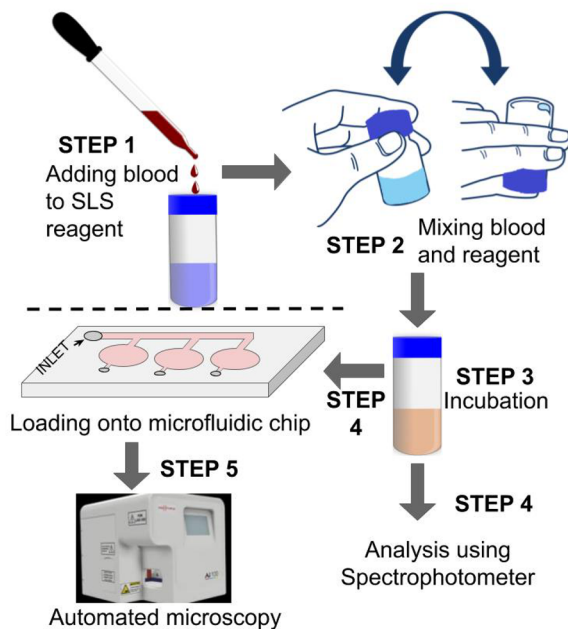
FIG. 3. Workflow for hemoglobin estimation using an automated microscope involved the following steps: Whole blood (50 μl, EDTA stabilized) was added to the SLS reagent (600 μl, 50× SLS) and mixed manually by shaking back and forth ten times; subsequently, the reagent–blood mixture was incubated for 10 min in the tube itself in case of analysis using nanospectrometer and biochemical analyzer, and in the case of on-chip estimation of hemoglobin using an automated microscope, the mixture was loaded after 5 min incubation, followed by 5 min on-chip incubation.

samples with higher hemoglobin concentrations were diluted 1:1 (dilution ratio) using PBS buffer. All blood samples were utilized in experiments within 48 h of collection. All refrigerated reagents and samples were allowed to equilibrate to ambient temperature for at least 30 min before conducting experiments. The finalized workflow for microscopy-based estimation, depicted in Fig. 3, involved the addition of 50 μl blood to 600 μl SLS reagent, subsequent ten times mixing, followed by 5 min incubation in a vial. After 5 min, the vial was mixed five times, followed by loading into three chambers of the microfluidic chip and left standing for 5 min. At the end of 5 min incubation, the chip was loaded onto a digital scanner device, and scanning was performed within 5 min.

III. RESULTS AND DISCUSSION

A. Effect of SDS concentration and Hb:SLS volume ratio, studied using Hb standard solutions (biochemical analyzer 546 nm)

In the conventional SLS hemoglobin assay, involving 1× SLS and blood:SLS reagent volume ratio 1:250, the concentration of the active ingredient (SDS, 2.5 mM) is significantly lower than the critical micellar concentration of SDS, which is 8.2 mM. As mentioned in the introduction section, in order to make the characteristics of blood:SLS reagent mixture suitable for low sensitivity detector, i.e.,

the camera, the volume ratio had to be modified and correspondingly the concentration of SDS in SLS reagent had to be increased. Therefore, it was necessary to understand the effect of elevated SDS concentration on the absorbance values at relevant wavelengths, and in this case, 546 nm was used in the semi-automated biochemical analyzer. Concentrations beyond 240× SLS were difficult to work with because of storage issues emanating from the SDS precipitating out of solution. The effect of SDS concentration on the value of absorbance measured using a biochemical analyzer is shown in Fig. 4. An internally prepared hemoglobin standard was used to perform this study. For constant blood:reagent volume ratio of 1:250, it was observed that the absorbance value decreased significantly for a given concentration of hemoglobin with the increase in SDS concentration. Relative to 1× SLS or 10× SLS, the average absorbance value for 100× SLS was lower by a factor of 1.5, and with 240× SLS, the absorbance value decreased by a factor of 3.4.

Despite the drop in absorbance, for a given SDS concentration, the linear relationship between absorbance and hemoglobin concentration was maintained. There are two important consequences of increasing the concentration of SDS in SLS reagent. First, a physical change is expected because of the formation of micelles, and it is well known that beyond the critical micellar concentration of SDS (8 mM), the anionic surfactant molecules self-assemble into micelles. Besides this, at higher concentrations of SDS (>20 mM), the conversion of hemoglobin to methemoglobin is further followed by conversion of methemoglobin into hemochrome like substance, whose absorbance at 535 nm is significantly lower than that observed with methemoglobin–SLS complex.[5] The cause of loss in signal with an increase in SDS concentration from 1× SLS to 100× or 240× SLS is the formation of hemochrome like substance whose extent of formation would be directly proportional to the concentration of SDS and hence a lower absorbance value for 240× SLS compared to 100× SLS.

In order to ascertain the extent of absorbance enhancement, the modified SLS assay involving higher s:SLS volume ratios of 1:25 and 1:5 were quantified using the biochemical analyzer. In order
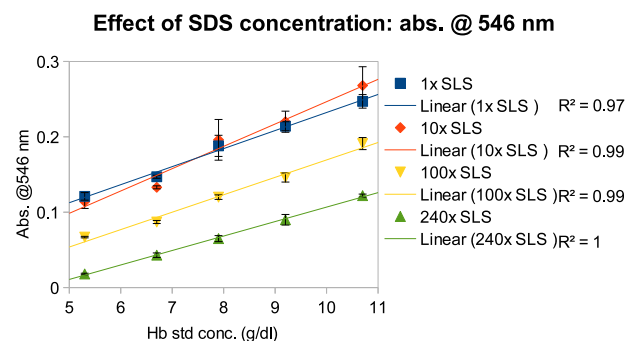

FIG. 4. Effect of increase in SDS concentration on the absorbance of hemoglobin standard–SLS reagent mixture (volume ratio 1:250) measured using biochemical analyzer (wavelength 546 nm). The measurement was performed within a 10 min–20 min time window after mixing hemoglobin standard with SLS reagent. Each data point is the average of triplicate measurements, and absorbance corresponds to 10 mm path length.
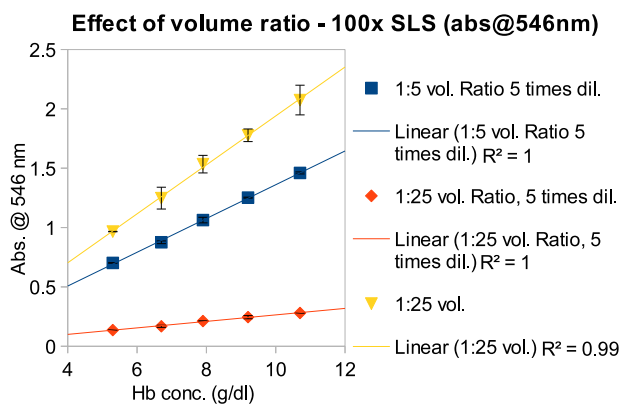
FIG. 5. Effect of increase in volume ratio from 1:250 to 1:5 or 1:25, studies using hemoglobin standards and 100× SLS reagent, measured using biochemical analyzer (wavelength 546 nm). In the case of 1:5 volume ratio, the solution was too dark causing signal saturation, thus requiring a five times dilution before measurement. The measurement was performed within a 10 min–20 min time window after mixing hemoglobin standard with SLS reagent. Each data point is the average of triplicate measurements, and absorbance corresponds to 10 mm path length.

to compensate for the significant increase in hemoglobin:SDS stoichiometric ratio associated with an increase in sample:SLS volume ratio, the concentration of SDS in SLS reagent was increased. Initially, 100× SLS and 240× SLS were studied, and the results of these studies are presented in Figs. 5 and 6, respectively.

Absorbance for volume ratio 1:5 was observed to saturate; hence, a further five times dilution (mixture:diluent volume ratio 1:4) was performed using PBS buffer. The dilution was performed just before measurement, and the measurement was performed
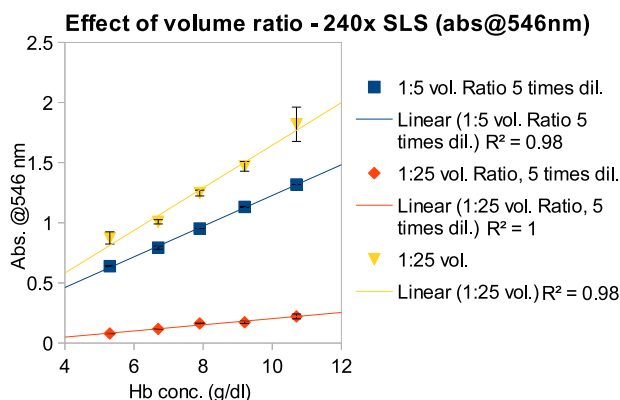

FIG. 6. Effect of increase in volume ratio from 1:250 to 1:5 or 1:25, studies using hemoglobin standards and 240× SLS reagent, measured using biochemical analyzer (wavelength 546 nm). In the case of 1:5 volume ratio, the solution was too dark, thus requiring a five times dilution before measurement. The measurement was performed within 10 min–20 min time window after mixing hemoglobin standard with SLS reagent. Each data point is the average of triplicate measurements, and absorbance corresponds to 10 mm path length.

within 1 min of diluent addition. Note that in order to perform a direct comparison between volume ratios 1:5 and 1:25, the absorbance values for 1:5 volume ratio was back-calculated from absorbance values measured after five times dilution. In the case of 100× SLS and 240× SLS, the absorbance for 1:5 dilution was higher than that for 1:25 dilution by an average factor of 5.1 and 6.6, respectively. This was expected based on the assumption that an increase in the concentration of SLS–hemoglobin complex with an increase in the sample:reagent volume ratio from 1:250 to 1:25 to 1:5 would result in a significant increase in absorbance in the green wavelength region relevant to SLS assay. Also, for a given hemoglobin concentration, the absorbance value observed with 100× SLS was higher than that observed for 240× SLS by an average factor of 1.4 and 1.1, for volume ratios 1:25 and 1:5, respectively. It is worth mentioning that volume ratio values higher than 1:5 were difficult to work with, because of the high viscosity of the resulting mixture, which necessitated prolonged vigorous mixing to ensure efficient mixing, as well as pipetting related issues. The assay format with a 1:5 volume ratio resulted in the maximum possible increase in absorbance value, and hence, this was chosen for further detailed studies to compare the modified assay with conventional SLS assay.

B. Comparison and characterization of modified SLS assay and conventional SLS assay

Once the volume ratio 1:5 was chosen, the corresponding concentration of SDS was calculated based on the stoichiometric ratio of SDS to hemoglobin (assuming the upper limit of hemoglobin to be 30 g dl^{-1}) in conventional SLS assay, which is 135. Upon calculation, this comes to be 50 times that of 1× SLS, i.e., 50× SLS (125 mM SDS). The absorbance measured using a biochemical analyzer (Erba Chem 5×, 546 nm) for three different hemoglobin standard solutions and the two different SLS reagents (1× SLS and 50× SLS) is presented in Fig. 7. For a given concentration of hemoglobin, the measured absorbance with 50× SLS was higher than that for 1× SLS by an average factor of 36. As a result of this huge gain in signal intensity, it becomes possible to significantly lower the path length of the measurement chamber (much needed for the adoption of SLS assay onto the microfluidic platform) and also enable the use of a low sensitivity detector such as a camera associated with blood smear autoanalyzers. Having estimated the quantitative signal enhancement, the next step involved comparing the spectral characteristics of newly developed SLS assay with those observed with conventional SLS assay using a nanospectrophotometer by performing a wavelength scan encompassing the Soret and Q bands.

In order to understand the chemical processes associated with the modified SLS assay, the mixture of hemoglobin standard or whole blood with 1× SLS and 50× SLS were analyzed over the wavelength range 400 nm–600 nm. This range is sufficient to obtain information about the two important spectral characteristics of hemoglobin–SLS interaction, namely, the Soret and Q band. The Soret band always consists of just one peak, while the Q band can have up to two peaks depending on whether oxygen/carbon-dioxide is bound to the hemoglobin molecule or not and depending on the oxidation state of Fe ion in heme, per reports by Zijlstra et al.[2,3] Mixtures of SLS (both 1× and 50) with whole blood as well as hemoglobin standard were scanned, and the summary of peak positions observed is presented in Table III. Representative scans for
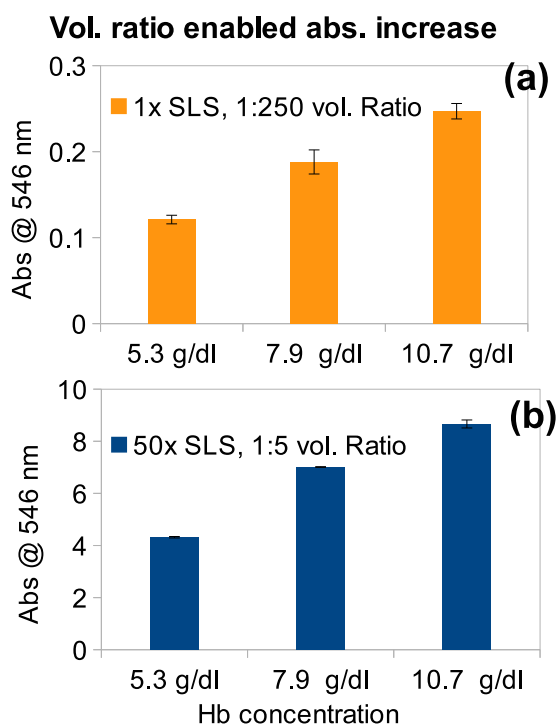
Vol. ratio enabled abs. increase

FIG. 7. Quantitative comparison of absorbance values obtained from biochemical analyzer (Erba Chem 5×, 546 nm) between reagents 1× SLS (a) and 50× SLS (b). Conventional SLS assay and modified SLS assays were compared using three different hemoglobin standard solutions. Each data point is the average of triplicate measurements, and absorbance corresponds to 10 mm path length.

each sample–reagent type are shown in Figs. 11 and 12 in the supplementary material. With hemoglobin standard, both controls (PBS 1:5 and 1:250) had Soret peak 406 nm and Q band (single peak) peak at 530 nm. The peak position of the Soret peak indicated

TABLE III. Peak positions of Soret and Q bands observed with hemoglobin standard and whole blood samples in combination with 50× SLS or 1× SLS reagent. As controls, PBS was used as a diluent instead of the SLS reagent. These wavelength scans were performed using nanospectrometer, and absorbance output always corresponded to 10 mm path length. Representative spectra associated with these peaks are presented in Figs. 11 and 12 in the supplementary material. The data presented for whole blood samples are an average of five different samples. The hemoglobin standard used had a Hb concentration of 10.7 g dl^{-1}.

Sample	Reagent used	Soret peak (nm)	Q band (nm)
Hb std.	1× SLS (1:250)	413	530
	PBS (1:250)	406	Not observed
	50× SLS (1:5)	413	530
	PBS (1:5)	406	Not observed
Blood	1× SLS (1:250)	414 ± 1	538 ± 1
	PBS (1:250)	414 ± 1	541 ± 1, 576 ± 1
	50× SLS (1:5)	414 ± 1	535 ± 1
	PBS (1:5)	415 ± 1	543 ± 1, 577 ± 1

that the lyophilized hemoglobin powder was predominantly methemoglobin like substance.[18] Upon addition of SLS to hemoglobin standard, the Soret peaks for both 1× SLS and 50× SLS shifted from 406 nm to 413 nm, which is indicative of the formation of SLS–Hb complex. In the case of experiments with whole blood samples diluted with PBS (both 1:5 and 1:250 volume ratios), two peaks were observed within the Q band, which indicated the presence of Fe ion in the Fe(II) oxidation state, per reports by Zijlstra et al.[2,3] After the addition of 1× SLS, the two distinct peaks of the Q band disappeared, and instead, a low-intensity peak was observed at 538 nm, indicating the conversion of hemoglobin into methemoglobin–SLS complex.[5] With 50× SLS, the Q band peak was observed at 535 nm. The 3 nm blue shift with 50× SLS relative to 1× SLS may be because of the formation of hemochrome from methemoglobin, which is expected due to a higher concentration of SDS in the case of 50× SLS reagent.[5] Overall, it can be concluded that the modified SLS reagent (50× SLS) introduces an additional chemical reaction to the conventional SLS assay, and the presence of a distinct peak at 535 nm very close to the peak associated with conventional assay indicates that the modified assay has the potential to provide quantitative information about the concentration of hemoglobin in whole blood by converting various forms of hemoglobin into a single form, namely, the hemochrome type substance. The next step would be to ascertain the quantitative relationship between the absorbance measured at 535 nm and the concentration of hemoglobin in whole blood samples, which is the topic of Sec. III C.

C. Ascertaining the quantitative performance of 50× SLS reagent using nanospectrophotometer

The conventional SLS assay using 1× SLS reagent is known to provide a linear relationship between absorbance measured in the Q band region and the concentration of hemoglobin in whole blood. As the modified SLS reagent is new, the relationship between measured absorbance and the concentration of hemoglobin across the clinically relevant range had to be established before implementing the modified assay on a microscopy platform. To start with, the quantitative relationship for 50× SLS reagent (1:5 volume ratio) between absorbance at 535 nm measured using a nanospectrophotometer, and hemoglobin concentration in hemoglobin standards was ascertained. The results of a correlation between measured absorbance and concentration of hemoglobin in hemoglobin standards are presented in Fig. 8.

Totally eight hemoglobin standard solutions with concentrations ranging between 5.3 g dl^{-1} and 18.6 g dl^{-1} were studied, and a linear relationship with a R^2 of 0.99 was observed between absorbance at 535 nm and concentration of hemoglobin. A similar study was performed using 25 whole blood samples whose hemoglobin concentrations were spread across the clinically relevant range. The study using blood also resulted in a linear relationship with an R^2 of 0.99. The absorbance values for hemoglobin standards were observed to be higher than those observed with blood by a factor of 1.8. As described in the Methods section, hemoglobin standards were prepared by reconstituting lyophilized hemoglobin powder, and the initially reconstituted solution had suspended aggregate particles, which settled down upon standing. It is possible that a significant number of particles remained suspended, while only the large particles settled down. These suspended particles may not

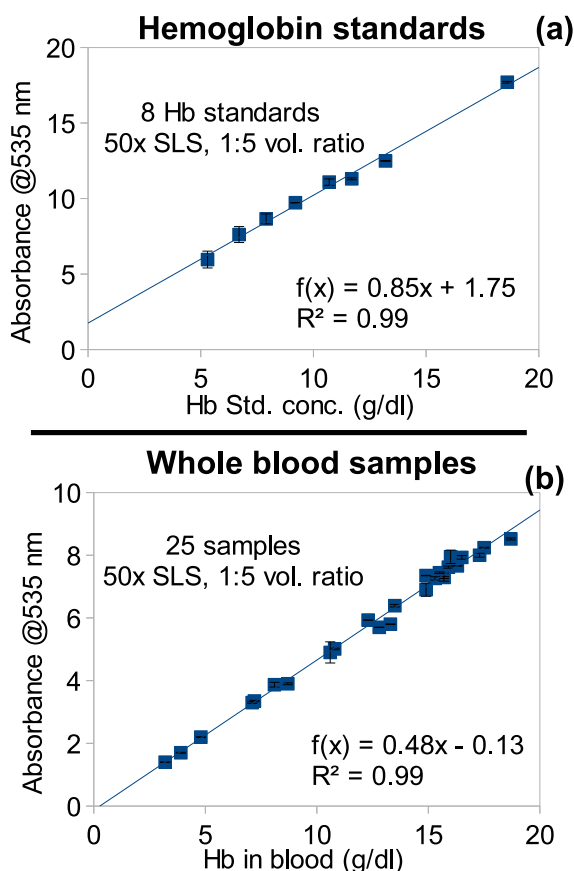## Correlation: Hb concentration and absorbance @ 535 nm

FIG. 8. Correlation between absorbance at 535 nm (y-axis) and concentration of hemoglobin (x-axis) measured using nanospectrophotometer with modified SLS assay involving 50× SLS reagent and 1:5 volume ratio. Eight hemoglobin standards with concentrations between 5.3 g dl^{-1} and 18.6 g dl^{-1} (a) and 25 blood samples in the range of 3.2 g dl^{-1}–18.7 g dl^{-1} (b).

get lyzed into individual hemoglobin–SLS complex molecules upon addition of 50× SLS reagent, which is not the case with RBCs in whole blood, which get completely lyzed out. The presence of suspended particles could contribute to a higher background, thereby causing the absorbance to increase significantly. The hemoglobin concentrations of standard solutions were estimated using the commercial hematology analyzer. The effect of the presence of suspended hemoglobin aggregate particles on the performance of the instrument is also something that might contribute to the observed differences between hemoglobin standard and whole blood samples. Overall, a linear relationship was observed between measured absorbance at 535 nm and concentration of hemoglobin in both whole blood and hemoglobin standards, thereby demonstrating that the modified SLS reagent (50× SLS) is a suitable reagent to provide the capability to quantitatively estimate the concentration of

hemoglobin in whole blood across a clinically relevant range of 0 g dl^{-1}–18 g dl^{-1}.

D. Hemoglobin estimation in whole blood using an automated microscope

After performing initial experiments on microscopy platform (only the green LED activated) with low, medium, and high concentration hemoglobin standard solutions (data not shown), using 100 μm, 250 μm, 500 μm, and 750 μm deep chambers, it was concluded that the maximum possible chamber depth of 1.3 mm (thickness of PMMA sheet 1.5 mm) was needed to get enough signal at low hemoglobin concentrations (<8 g dl^{-1}). However, at this depth, the high concentration hemoglobin solutions (>14 g dl^{-1}) resulted in saturation of the signal. In order to mitigate this saturation, the volume ratio was varied from 1:5 to 1:8 and 1:12 (data not shown). It was concluded that a 1:12 volume ratio using 50× SLS was ideal to enable quantitative estimation of hemoglobin across the entire clinical range. A transition from 1:5 to 1:12 would result in an SDS concentration change from 104 mM to 115 mM in the final mixture, which would not affect the nature of chemical reactions between SDS and hemoglobin.[5] As described in the Methods section, the microfluidic device was made out of a 1.5 mm thick PMMA sheet and each device contained three chambers for triplicate measurements. The device design features including the height and diameter of the chamber, height of inlet and outlet channels relative to connecting channel, as well as chamber height were paramount to the filling of chambers without air columns.

Besides the microfluidic device parameters, other optical setup related parameters associated with the e-con camera as listed in the Methods section were also optimized through preliminary studies. Once all these parameters were finalized, a clinical validation study was performed to check if a modified reagent in combination with the microfluidic device on a microscopic platform is capable of estimating hemoglobin in blood samples across the clinically relevant range. Preceding the clinical validation was a study to deduce the calibration equation to convert the grayscale values recorded using the microscopy camera into hemoglobin concentration. This experimental deduction was performed using 25 blood samples. To start with, the grayscale values in the green channel for 25 samples were measured using 50× SLS, 1:12 volume ratio, three-chamber microfluidic chip on an automated microscopy platform. As the true hemoglobin concentrations of these blood samples and the path length (0.13 cm) were known, these measured grayscale values were used in the below mentioned rearranged Beer–Lambert's law to calculate the molar extinction coefficient for Hb–SLS hemochrome type substance using this particular setup consisting of green LED illumination in combination with e-con camera,

$$Ext.\ coefficient = \frac{\log \frac{Io}{I}}{Pathlength \times Hb\ conc.}, \qquad (5)$$

where I is the gray level value obtained from three chambers, and Io the pre-measured value corresponding to gray level obtained from chambers filled with SLS reagent (no blood). Here, the extinction coefficient, path length, and concentration have the units dl g^{-1} cm^{-1}, cm, and g dl^{-1}.

A similar extinction coefficient calculation was performed using the absorbance data from nanospectrophotometer measurements at 535 nm in Sec. III C, where 25 blood samples were analyzed with a standard path length of 1 cm. Note that the extinction coefficient calculations from absorbance as well as grayscale values were performed only after normalizing the effect of the difference in dilution ratios resulting from varying volume ratios. Both these routes of calculating extinction coefficients resulted in nearly the same values of 2.797 (CV% 14.2) and 2.794 (CV% 3.4) dl g^{-1} cm^{-1} using automated microscopy (grayscale) and nanospectrophotometer (absorbance), respectively. This was surprising considering the fact that the green LED used for illumination in the automated microscope has a peak at 520 nm, while the peak of hemochrome formed during 50× SLS hemoglobin interaction has an absorption peak at 535 nm. Perhaps the broad optical bandwidth of green LED could be responsible for sufficient illumination at 535 nm.

One additional important observation was the considerably higher percentage coefficient of variation in the case of extinction coefficient calculated from microscopy setup (CV% 14.2) when compared to that obtained from nanospectrophotometer (CV% 3.4) measurements. For example, in the case of automated microscopic measurement, blood samples with hemoglobin concentrations of 4 g dl^{-1} and 17.7 g dl^{-1} gave extinction coefficients of 2.1 dl g^{-1} cm^{-1} and 3.5 dl g^{-1} cm^{-1}, respectively. On the other hand, in the case of measurements using nanospectrophotometer, blood samples with hemoglobin concentrations of 3.2 g dl^{-1} and 17.5 g dl^{-1} gave extinction coefficients of 2.6 dl g^{-1} cm^{-1} and 2.8 dl g^{-1} cm^{-1}, respectively. This indicates that the variation in apparent extinction coefficient in the case of automated microscopy setup originates mainly from the non-linear response of the camera as a function of intensity, which in turn varies linearly as a function of hemoglobin concentration, as demonstrated by the linear relationship between absorbance at 535 nm and hemoglobin concentration (Fig. 8). Because of variation in extinction coefficient, an average extinction coefficient of 2.797 was considered for calculating hemoglobin concentration from microscopy measured grayscale values using the Beer–Lambert's law as mentioned in Eq. (2).

The experimentally determined extinction coefficient was used to convert the grayscale values measured by automated microscope into hemoglobin values for 25 blood samples in the preclinical study using Eq. (2). The thus obtained hemoglobin values of blood samples estimated using automated microscopy setup were correlated with true hemoglobin concentrations obtained from commercial Sysmex hematological analyzer. A power correlation [Eq. (3)] was found to be the best fit, as shown in Fig. 9, giving an R^2 of 0.98. Thus, this relationship would convert the hemoglobin values calculated using Beer–Lambert's law into actual clinically relevant hemoglobin values, which would be the final output.

Overall, the preclinical study resulted in a two-step procedure to convert automated microscopy measured grayscale values into intermediate hemoglobin concentrations using Eq. (2), which were further converted into final hemoglobin concentrations using Eq. (3). This two-step procedure was clinically verified using 27 blood samples, wherein the automated microscopy derived grayscale values were input into Eq. (2) and the resulting intermediate hemoglobin concentration was input into Eq. (3). The final hemoglobin concentrations at the end of the two-step
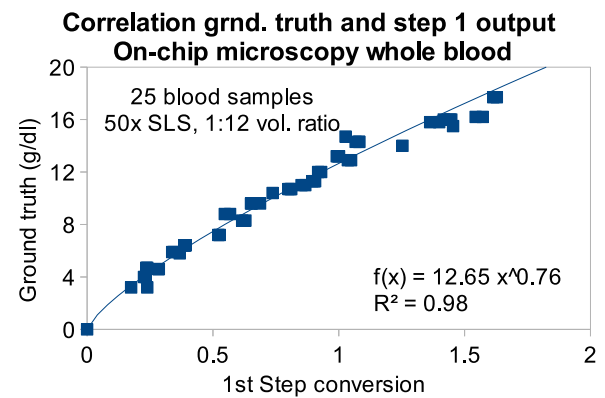

FIG. 9. Correlation between intermediate hemoglobin concentrations of 25 blood samples calculated from automated microscopic grayscale values using Beer–Lambert's law and true hemoglobin concentrations measured using commercial hematology analyzer. The best curve fit was obtained using the power function.

procedure were correlated with true hemoglobin concentrations measured using a commercial hematology analyzer, as shown in Fig. 10. Besides the correlation coefficient, the performance of the newly developed assay was ascertained by clinical accuracy assessment (with reference to Table II). Correlation results along with clinical performance data are presented in Table IV. A linear relationship with an R^2 of 0.99 and a Pearson correlation of 0.99 was obtained. This indicates a high correlation between the newly developed assay and a commercially available (clinically validated) assay. The clinical performance of any assay is ascertained based on calculating sensitivity and specificity. To start with, the samples are classified into negatives and positives, with respect to the state of normal or abnormal according to the ranges mentioned in Table II. Sensitivity is the ratio of the number of true positives to the sum of true positives and false negatives. Specificity is the ratio of the number of true negatives to the sum of true negatives and false positives. The newly developed method achieved a sensitivity of 92.3%, which
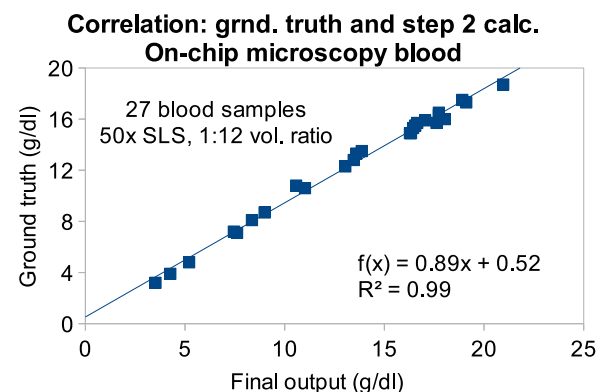

FIG. 10. Correlation between final hemoglobin value determined from automated microscopy method and the true hemoglobin concentrations of 27 blood samples measured using commercial hematology analyzer, Sysmex XP-100.

TABLE IV. This is a summary of the correlation between final hemoglobin concentrations of 25 blood samples determined by automated microscopy and a commercially available hematology analyzer. Additionally, the clinical performance results including sensitivity and specificity are presented.

Performance parameter	Value
Clinical sensitivity	92.3%
Clinical specificity	53.8%
Outliers (>10% deviation)	15%
Pearson correlation	0.99
R^2	0.99

is satisfactory. This method had poor specificity of 53.8%. There are several areas where improvements could be implemented, for example, the chip to chip variation arising from milling based fabrication process resulting in variation in chamber depth and also randomly formed milling marks, which can be minimized if the chips were to be fabricated through the injection molding process. Also, the volumetric errors arising from manual pipetting of SLS reagent and blood would lead to deviation from ground truth. These errors could be mitigated through the usage of automated liquid dispensers or high accuracy fixed volume pipettes.

E. Discussion

As mentioned earlier, each packaged microfluidic device along with a reagent meant for a single hemoglobin measurement would have a bill of materials (BOM) totaling 0.136 USD. The breakup of the total cost into individual components is presented in Table V. The PMMA device constituted a major part of the total cost, ~40%. Also, the cost of a microfluidic chip is estimated based on the assumption that it would be mass-produced via an injection molding process, instead of the currently used prototyping process of milling. It must be mentioned that the final list price would be significantly higher, usually at least by a factor of 2–4. There are numerous stand-alone quantitative hemoglobin tests demonstrated in research reports and also available in the market, which are more cost-effective and also performance-wise superior.[19,20] For example, the price of each strip (microcuvettes) used in a Hemocue 301 is 0.4 USD, while the BOM for the strip developed by Yang *et al.* was

TABLE V. Breakup of the total cost of the microfluidic device including reagent, vial, packaging, and labeling.

Component	Cost in USD
PMMA chip	0.05
Cover-film	0.014
Reagent vial	0.014
Liquid reagent	0.007
Labeling and packaging	0.029
Manufacturing	0.029
Total	0.136

<0.007 USD.[19,20] Nevertheless, the relevance of this particular assay developed in conjunction with an automated microscope becomes clear upon considering the integrated chip. The integrated chip would consist of multiple microfluidic chambers on a single chip, thereby allowing the determination of hemoglobin concentration, WBC differential count, as well as total count, total count of RBC, and platelet count. It is well known that upon the quantitative estimation of hemoglobin, it becomes possible to calculate additional parameters such as Mean Corpuscular Hemoglobin (MCH), Mean Corpuscular Hemoglobin Concentration (MCHC), and Hematocrit number (HCT).[21] Thus, this integrated chip would be capable of providing complete blood count using an imaging-based platform (automated microscope), which would have a significantly lower cost when compared to commercial autoanalyzers. The details about the integrated device and its performance will be presented as part of a separate research report, which is at present under preparation. The imaging-based hemoglobin assay being reported here is a highly relevant necessity when it comes to developing cost-effective alternatives to the most prevalent hematology analyzers.

IV. CONCLUSIONS

An imaging-based hemoglobin estimation setup was developed in conjunction with a microfluidic chip and an AI-powered automated microscope designed for deriving total as well as differential counts of blood cells. The SLS method was chosen as the biochemical route, and the parameters such as the concentration of SDS and blood to reagent volume ratio were optimized to be 125 mM and 1:12, respectively, so as to enable quantitative estimation of hemoglobin in whole blood samples using a microfluidic chip with a maximum allowable path length of 1.3 mm. The automated microscope, which normally uses a combination of the red, green, and blue LED, used just the green LED during the hemoglobin estimation mode, and additionally, the grayscale values from the green channel of the image generated by an e-con camera with optimized parameters, including exposure time, gain, white balance, and local tone mapping, were found to result in a setup capable of measuring hemoglobin in the blood, which was demonstrated through a clinical verification with 27 blood samples. The newly developed method was able to achieve a Pearson correlation of 0.99 with a commercial autoanalyzer, Sysmex XP-100. Additionally, a clinical sensitivity of 92.3% and a specificity of 53.8% were achieved using this method. Besides performance evaluation, the biochemical aspects of the newly developed SLS reagent in combination with the altered volume ratio, especially the nature of the SLS hemoglobin complex formed, was characterized using spectroscopic studies, which indicated the formation of hemochrome-like substances.

SUPPLEMENTARY MATERIAL

See the supplementary material for representative UV–vis spectral scans of the mixture of blood or hemoglobin standard with conventional as well as customized SLS reagents, along with time-lapse images of the microfluidic chip being filled with the reagent–sample mix.

DATA AVAILABILITY

The data that support the findings of this study are available from the corresponding author upon reasonable request.

REFERENCES

[1] A. V. Hoffbrand, *Essential Haematology*, 3rd ed. (Wiley-Blackwell, Oxford, 1993).
[2] W. G. Zijlstra *et al.*, Comp. Biochem. Physiol., Part B **107**, 161 (1994).
[3] W. G. Zijlstra and A. Buursma, Comp. Biochem. Physiol., Part B **118**, 743 (1997).
[4] S. M. Lewis *et al.*, Clin. Lab. Haematol. **13**, 279 (1991).
[5] I. Oshiro *et al.*, Clin. Biochem. **15**, 83 (1982).
[6] E. J. Wang, "HemaApp: Noninvasive blood screening of hemoglobin using smartphone cameras," in *Proceedings of the 2016 ACM International Joint Conference, September 12, 2016* (Association for Computing Machinery, New York, NY, 2016), pp. 593–604.
[7] M. D. Anggraeni and A. Fatoni, IOP Conf. Ser.: Mater. Sci. Eng. **172**, 012030 (2017).
[8] T. Srivastava, J. Hematol. Transfus. **2**, 1028 (2014).
[9] J. Steigert *et al.*, Sens. Actuators, A **130-131**, 228 (2006).
[10] C. Wu, in *Conference on Neural Information Processing Systems* (NIPS, 2017), Vol. 1712, p. 00174.
[11] K. Chu *et al.*, Expert Rev. Med. Devices **12**, 613 (2015).
[12] E. Mieczkowska *et al.*, Anal. Bioanal. Chem. **399**, 3293 (2011).
[13] N. Taparia *et al.*, AIP Adv. **7**, 105102 (2017).
[14] H. Zhu *et al.*, Lab Chip **13**, 1282 (2013).
[15] M. Azhar *et al.*, IEEE Trans. Biomed. Eng. **67**, 1243 (2020).
[16] T. R. Dastidar and R. Ethirajan, Biomed. Opt. Express **11**, 480 (2020).
[17] H. Bruus, *Theoretical Microfluidics* (Oxford University Press, 2008).
[18] H. Sakai *et al.*, Bioconjugate Chem. **15**, 1037 (2004).
[19] X. Yang *et al.*, Clin. Chem. **59**, 1506 (2013).
[20] F. Sanchis-Gomar *et al.*, J. Lab. Autom. **18**, 198 (2012).
[21] K. Doig and M. Butina, Am. Soc. Clin. Lab. Sci. **30**, 173 (2017).